Original Article

On-line near-infrared spectroscopy optimizing and monitoring biotransformation process of γ-aminobutyric acid ☆

Guoyu Ding, Yuanyuan Hou *, Jiamin Peng, Yunbing Shen, Min Jiang, Gang Bai

State Key Laboratory of Medicinal Chemical Biology, College of Pharmacy, Nankai University; Tianjin Key Laboratory of Molecular Drug Research, Nankai University, Tianjin 300071, China

ABSTRACT

Near-infrared spectroscopy (NIRS) with its fast and nondestructive advantages can be qualified for the real-time quantitative analysis. This paper demonstrates that NIRS combined with partial least squares (PLS) regression can be used as a rapid analytical method to simultaneously quantify L-glutamic acid (L-Glu) and γ-aminobutyric acid (GABA) in a biotransformation process and to guide the optimization of production conditions when the merits of NIRS are combined with response surface methodology. The high performance liquid chromatography (HPLC) reference analysis was performed by the *o*-phthaldialdehyde pre-column derivatization. NIRS measurements of two batches of 141 samples were firstly analyzed by PLS with several spectral pre-processing methods. Compared with those of the HPLC reference analysis, the resulting determination coefficients (R^2), root mean square error of prediction ($RMSEP$) and residual predictive deviation (RPD) of the external validation for the L-Glu concentration were 99.5%, 1.62 g/L, and 11.3, respectively. For the GABA concentration, R^2, $RMSEP$, and RPD were 99.8%, 4.00 g/L, and 16.4, respectively. This NIRS model was then used to optimize the biotransformation process through a Box-Behnken experimental design. Under the optimal conditions without pH adjustment, 200 g/L L-Glu could be catalyzed by 7148 U/L glutamate decarboxylase (GAD) to GABA, reaching 99% conversion at the fifth hour. NIRS analysis provided timely information on the conversion from L-Glu to GABA. The results suggest that the NIRS model can not only be used for the routine profiling of enzymatic conversion, providing a simple and effective method of monitoring the biotransformation process of GABA, but also be considered to be an optimal tool to guide the optimization of production conditions.

© 2016 Xi'an Jiaotong University. Production and hosting by Elsevier B.V. This is an open access article under the CC BY-NC-ND license (http://creativecommons.org/licenses/by-nc-nd/4.0/).

1. Introduction

γ-aminobutyric acid (GABA) is an important non-protein component amino acid that is applied in various fields such as food [1], medical healthcare [2], and chemical engineering [3]. GABA has received growing attention in the medical healthcare field due to its inhibitory effects on central nervous system, including sedation, anti-depression, anti-insomnia, anti-hypertensive and diuretic effects [4–6]. It can be produced by several methods such as plant tissue enrichment [7], microbial fermentation [8] and biotransformation [9], and can be transformed by *Escherichia coli* (*E. coli*), genetically engineered strain expressing high levels of glutamate decarboxylase (GAD, EC4.1.1.15). By the enzymatic synthesis strategy (Fig. 1), the production of GABA

has higher concentration and purity. Although the amino acid enzymatic conversion strategy is easy to operate, it is not possible to ensure that the enzymatic activity remains constant, as strain passage and culture conditions can lead to some differences. If the enzymatic activity is too high, it will be a waste of the enzyme using the same biomass. When the enzymatic activity is too low, the transformation rate will decrease, which decreases the product purity and production efficiency due to the unclear endpoint of the biotransformation process [10]. Therefore, a proper process-monitoring method is beneficial for the programmed production of GABA.

Processional analytical technology (PAT) is defined as "systems for continuous analysis and control of manufacturing processes based on real-time, or rapid measurements during processing, of quality and performance attributes of raw and in-process materials and processes to ensure end product quality at completion of the process" by the United States Food and Drug Administration (USFDA). To ensure product quality, FDA suggests that the introduction of PAT can provide quality control during processing,
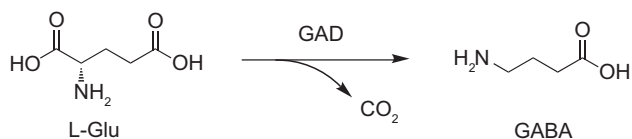

Fig. 1. Reaction equation of biotransformation from L-Glu to GABA.

including control over raw and in-process materials and processes to ensure end product quality at the end of the process. In particular, near-infrared spectroscopy (NIRS) is an advanced analytical technology that has recently been highly developed in the PAT field [11–13]. Because NIRS has many merits such as simple operation (no sample pretreatment), rapid measurement, no pollution, providing a large amount of information (physical and chemical properties can be determined with simple one time scanning and without damaging samples) [14]. Due to these advantages, NIRS has been introduced to the pharmaceutical, food, chemical engineering, textile, petroleum, and vintage industries [15–21]. For example, NIRS was investigated as a PAT to monitor amino acid concentration profiles during the hydrolysis of Cornu Bubali [22]. In this research, a NIRS model was developed using interval partial least squares and synergy interval partial least squares to monitor 11 different amino acids. A new parameter desirability index and multivariate quantification limit (MQL) values were used to evaluate the NIRS model. Excellent accuracies and low MQL values were obtained for L-proline, L-tyrosine, L-valine, L-phenylalanine and L-lysine. The results confirmed that these models are suitable to improve hydrolysis efficiency, and enabled a reduction in hydrolysis time, which directly affects process productivity.

Almost all types of compounds and mixtures can be quantified by NIRS with the chemometrics method. In this study, the optimization of the GABA enzymatic synthesis and monitoring of the biotransformation process both required multiple points testing and rapid results feedback. NIRS with its fast and nondestructive advantages will be qualified for the real-time quantitative analysis. It can provide guidance to determine whether the production process of GABA biotransformation is performing consistently with expectations, and rapid analysis at the end of the biological reaction. In this study, multivariate models were developed to quantify L-Glu and GABA levels that had previously been determined by pre-column derivatization high performance liquid chromatography (HPLC), and then partial least squares (PLS) regression prediction models with NIRS were constructed. After evaluating the stability, a new batch of samples was used for external validation to monitor biotransformation. Then, a Box-Behnken experimental design was used to optimize the process parameters using the NIRS model. Finally, the best process conditions were used for the GABA biotransformation process with on-line NIRS monitoring.

2. Materials and methods

2.1. Instruments

Analysis was carried out on an Agilent–1200 HPLC system (Agilent Technologies, Waldbronn, Germany) equipped with a quaternary pump (G1311C), on-line degasser (G1322A), auto-sampler (G1229A), thermo column compartment (G1316A) and photo-diode-detector (G4212A). Near-infrared diffuse reflectance spectra were acquired using a Bruker TENSOR 37 FT-NIR spectrometer (Bruker Optik, Ettlingen, Germany) with an InGaAs detector and an Integrating Sphere Module over the wavenumber range of 12,000–4000 cm^{-1}.

The biotransformation process was carried out in a 15 L glass tank bioreactor (Applikon Biotechnology, Delft, the Netherlands). The GAD genetically engineered super producer *E. coli* strain was cultivated in a 150 L fermenter (Biotech–2002 Bioprocess Controller, Baoxing, Shanghai, China).

2.2. Chemicals and materials

HPLC-grade acetonitrile and methanol were purchased from Merck (Darmstadt, Germany). Deionized water was prepared by a Milli-Q water system (Millipore, Bedford, MA, USA) to prepare samples and the mobile phase. Other reagents were of analytical grade, and were purchased from Concord Technology (Tianjin, China). All solvents were filtered through 0.22 μm membrane filters before analysis.

The reference standards (GABA and L-Glu) and the coenzyme pyridoxal 5′-phosphate (PLP) were obtained from Sigma-Aldrich (St. Louis, MO, USA). The purities of all of the standards were not less than 98%. The L-Glu, yeast extract and tryptone used in fermentation and biotransformation were purchased from Teda Letai Chemical Co., Ltd (Tianjin, China).

2.3. Cultivation of genetically engineered strain

The GAD high-expression strain of *E. coli* BL21 (NK-GAD402) was obtained from earlier work in our laboratory. The *E. coli* strain (NK-GAD402) was grown at 37 °C in a fermenter with 100 L of nutrient medium with the following composition: 5.0 g/L of yeast extract, 10 g/L of NaCl, 10 g/L of tryptone and up to 65 L of tap water (pH 7.2). The mixer rotation speed was 300 rpm, and the flow rate of sterile air was 15 L/min. When the optical density of the culture medium reached 1.0 at 600 nm, approximately 5 L of a 200 g/L lactose solution was fed into the fermentation broth. After 4 h of lactose induction, approximately 500 g of the GAD high-expression strain was obtained through centrifugation (3000 rpm). The obtained biomass was redissolved in water to obtain a concentration of 200 g/L and frozen at −20 °C.

The enzymatic activity of GAD was expressed in U/g cells (wet weight) and determined according to a previously developed method with slight modification [23]. One unit (U) of GABA-forming activity was defined as the amount of enzyme that liberates 1 μM GABA per minute in the following activity assay mixture. To start the reaction, 5 mL of 10 mg/mL biomass (wet weight) was added into the reaction mixture containing 35 g/L sodium glutamate, 200 mM Macilvaine buffer and 0.02 mM PLP at pH 4.35. After incubation at 37 °C for 30 min, the reaction was terminated by dilution in boric acid buffer (0.4 M, pH 10.2). The supernatant was obtained by centrifugation at 12,000 rpm for 10 min at room temperature and was then subjected to HPLC analysis.

2.4. Biotransformation of L-glutamic acid

Improving the cell wall permeability can increase the chance of substrate access to intracellular enzymes, increasing the conversion efficiency. To undergo thermal activation, the strain NK-GAD402 biomass was stored in a −20 °C freezer and then pre-incubated in a 37 °C water bath before use. L-Glu (2 kg) and PLP (50 mg) were then added into 10 L of water. Initially, 1200 U/L GAD high-expression strain (NK-GAD402) and 1 mL organic foam suppressor were added to the reaction environment. One hour later, fed-batch processing began at 660 U/L/h biomass, lasting for 8 h. The first sample was collected after 20 min. From that time on, samples were obtained every 10 min up to 12 h from the beginning of reaction. A total of 141 samples were obtained from two fermentation trials. The first batch of samples was used for

calibration, and the second for validation.

2.5. Preparation of standard and sample solutions

To determine the concentration of L-Glu and GABA in the bio-transformation process, 100 μL sample was collected from the bioreactor, diluted with 25 or 50 mL boric acid buffer (0.4 M, pH 10.2) to stop the enzymatic reaction, and prepared for HPLC analysis.

L-Glu and GABA reference compounds were accurately weighed, dissolved in 1% hydrochloric acid, and diluted to an appropriate concentration with the boric acid buffer. A mixed standard solution was prepared in 1% hydrochloric acid. All solutions were stored in a refrigerator at 4 °C and allowed to warm to room temperature before analysis. The o-Phthaldialdehyde (OPA) solution was prepared by mixing 100 mg of OPA, 9 mL of boric acid buffer, 1 mL of acetonitrile and 130 μL of 2-mercaptoethanol. After mixing, the OPA solution was passed through a 0.45 μm syringe filter.

2.6. Derivatization procedure and chromatographic conditions

Solution A was prepared with 0.8 g/L sodium acetate and 0.022% triethylamine in water, adjusted to pH 7.20 ± 0.05 with 5% (v/v) acetic acid. And the sodium acetate buffer was prepared with 0.8 g/L sodium acetate in water, adjusted to pH 7.20 ± 0.05 with 2% (v/v) acetic acid. Solution B was blended together at the ratio of 2:2:1 with acetonitrile, methanol and the sodium acetate buffer.

The auto-sampler was programmed to mix 20 μL standard or sample solution with 1 μL of the OPA reagent solution and 9 μL of boric acid solution for 1 min in the derivatization loop. After the OPA mixtures were injected into the HPLC column, a solvent gradient was initiated.

The analysis was performed on a Phenomenex Luna reversed-phase C_{18} column (250 mm × 4.6 mm, 5 μm) and maintained at 25 °C. The mobile phase was a mixture of solution A and solution B according to the following gradient: 0 min, 20% B; 3 min, 30% B; 7–12 min, 100% B; and 14–17.3 min, 20% B. Elution was performed at a solvent flow rate of 1.0 mL/min, and chromatograms were collected at 338 nm by the PDA detector. The injection volume was 10 μL for each sample and standard solution.

2.7. Multivariate calibration model

2.7.1. NIRS

NIRS were acquired using a Brucker TENSOR 37 FT-NIR spectrometer (Bruker Optik, Ettlingen, Germany) over the wavenumber range of 12000 to 4000 cm^{-1}. A cuvette of 2 mm thickness was applied for the transmission spectrum research with a resolution of 8 cm^{-1} by averaging over 32 scans. Temperature and relative humidity remained approximately 23 °C and 55%, respectively. A background spectrum was collected for water. Triplicate spectra were collected consecutively for each sample.

2.7.2. Spectral pre-processing

To achieve the best prediction performance, several spectral pre-processing techniques were investigated using the Bruker TENSOR 37 SYSTEM OPUS 7.0 Edition (Bruker Optics, Ettlingen, Germany). The spectral pre-processing methods included constant offset elimination, straight line subtraction, standard normal variate transformation (SNV), min–max normalization, multiplicative scatter correction (MSC), first derivative (Der1), second derivative (Der2), Der1+straight line subtraction, Der1+SNV and Der1+MSC.

2.7.3. PLS calibration

PLS regression is a powerful method of revealing the linear relationship between spectra (X) and parameters under investigation (Y) [24]. During PLS analysis, both X and Y matrices are first transformed into new spaces, and the obtained X and Y scores are then carefully selected and correlated in an attempt to maximize the interpretation of Y scores based on X scores. Subsequently, the predicted Y scores are used to predict Y. Collected spectra were analyzed using PLS regression analysis built-in OPUS 7.0. To select the calibration model parameters including the number of PLS factors and the pre-processing method, optimal conditions were determined for the calibration set with the lowest root mean square error of cross validation (RMSECV). Once these conditions were determined for the calibration set, the validation samples were returned to the calibration set, and the same calibration parameters were used to establish PLS models. As a validation set is employed, model parameters are independent of the external validation data set, which should produce more robust calibration models that are less dependent on the specific samples employed. Each sample spectrum was collected in triplicate to reduce any machine dependent effects.

The spectra from the first batch of biotransformation were sorted by sampling time for the 71 samples used as a calibration set. All of the 70 samples from the second batch were used as a validation set.

2.7.4. Model assessment

To assess the model developed here, determination coefficients (R^2), RMSECV, residual predictive deviation (RPD) and root mean square error of prediction (RMSEP) were computed to evaluate the performance. These parameters are defined as follows:

$$R^2 = 1 - \frac{\sum_{i=1}^{n}(y_{i,predicted} - y_{i,actual})^2}{\sum_{i=1}^{n}(y_{i,predicted} - y_{average})^2} \tag{1}$$

$$RMSECV = \sqrt{\frac{\sum_{i=1}^{n}(y_{i,predicted} - y_{i,actual})^2}{(n-1)}} \tag{2}$$

$$RMSEP = \sqrt{\frac{\sum_{i=1}^{m}(y_{i,predicted} - y_{i,actual})^2}{(m-1)}} \tag{3}$$

$$RPD = \frac{SD}{RMSEP} \tag{4}$$

where $y_{i,predicted}$ is the predicted Glu/GABA result, $y_{i,actual}$ is the Glu/GABA reference result, and $y_{average}$ represents the average of the reference results of all samples. n is the number of samples for calibration and m is the number of samples for validation or external validation. SD is the standard deviation of the reference results of all samples in the validation.

2.8. Box-Behnken design

Design expert 7.0 software was used to generate the matrix and analyze the response surface models. A 3-level, 3-factor Box-Behnken design was selected for this study because it can evaluate quadratic interactions between pairs of factors while minimizing the number of required experiments. The influences of interactions among three factors, i.e., total enzymatic activity, total time of enzyme addition and reaction time, were examined in this study. A total of 17 experiments were performed to test the effects of these factors. The two responses (GABA content and the initial

Table 1
Factors and levels for the Box-Behnken experimental design.

Factors	Code	Level		
		−1	0	1
Total enzymatic activity (U/L)	A	3330	6660	13,320
Total time of enzyme addition (h)	B	1.5	3	6
Reaction time (h)	C	3	4	5

GABA concentration in the first hour) were measured for each experiment. The coded design patterns represent the scaled factor values (high (1), middle (0) and low (−1)) used in each run, in the order of total enzymatic activity, total time of enzyme addition and reaction time, respectively (Table 1). The responses were predicted by the NIRS model constructed in Section 2.5.

To verify the reliability of the resulting model, tests were performed using the optimal process parameters. This third batch acted as the model validation.

3. Results and discussion

3.1. HPLC analysis of L-Glu and GABA

With the developed pre-column derivatization HPLC method, L-Glu and GABA were separated and identified according to their retention time (Fig. 2); good linearity of each marker component was observed over a relatively wide concentration range (0.005–0.2 g/L) with a correlation coefficient above 0.99, and the limit of determination (LOD) and limit of quantitation (LOQ) are also listed in Table 2. The precision, reproducibility, and accuracy of this method were also satisfactory.

3.2. Raw and pre-processing spectral analysis

Fig. 3A presents the raw NIR spectra of samples taken from the GABA biotransformation at wavenumbers ranging from 9000 to 4000 cm^{-1}. After Der1 pretreatment of the raw NIR spectra, several characteristic absorption peaks can be observed in Fig. 3B, including 8780 and 8600 cm^{-1} due to the second overtone of the C–H stretching vibration and the combination of the first overtone of the C–H stretching and deformation vibrations; 7180 cm^{-1} due to the combination of the first overtone of the C–H stretching and C–H fundamental deformation vibrations; 6790 cm^{-1} due to the first overtone of the N–H stretching vibration; 6000, 5940, 5820, 5800, and 5650 cm^{-1} due to the first overtone of C–H stretching; 4640 cm^{-1} due to the combination of N–H fundamental stretching and deformation vibrations; and 4480, 4400, and 4340 cm^{-1} due
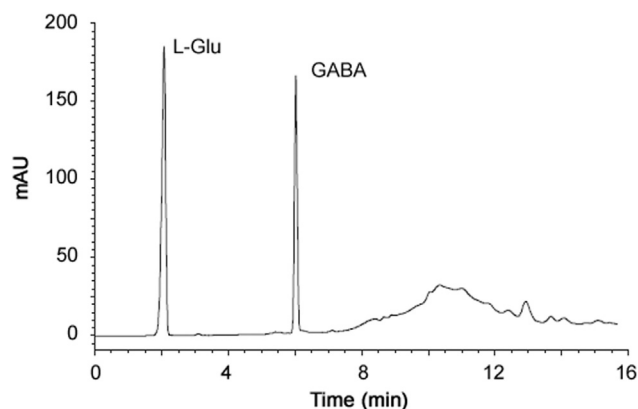

Fig. 2. HPLC profiling of a mixed standard solution.

Table 2
Calibration curves of L-Glu and GABA.

Analytes	Calibration curve	R^2	Linear range (g/L)	LOQ (g/L)	LOD (g/L)
L-Glu	$Y = 53{,}267X - 40.076$	0.9989	0.005–0.2	0.0015	0.0005
GABA	$Y = 41{,}666X - 3.186$	0.9987	0.005–0.2	0.0024	0.0008

to the combination of C–H fundamental stretching and deformation vibrations [25–27]. These signals could arise from CH_2 and NH_2 bonds in L-Glu and GABA, the two main compounds in the broth, indicating that NIRS can reflect the chemical information of the samples and monitor the biotransformation process.

3.3. Development of a PLS multivariate calibration model

Multivariate calibration models have several important parameters, including wavelength range, spectral pretreatment method and latent variables (LVs). Generally, optimal model parameters depend on the lowest *RMSEP* and higher *RPD* with lower *LVs*. In this study, automatic optimization software (OPUS 7.0) was used to obtain the best model by an optimized spectral pretreatment method, with LVs over the wavelength range without noise components (12,000–5300 and 4872–4224 cm^{-1}). The optimization results showed that the traditional spectral pretreatments, SNV and MSC, were not suitable for the development of a multivariate calibration model to determine L-Glu and GABA in the biotransformation process (Table 3). As SNV and MSC are used to eliminate the scattering effects produced by heterogeneous distributions and irregular particle forms, they are normally used to analyze the diffuse reflection of solid samples and the transmission reflection of slurry substances [28]. Different pretreatments were tested. The adopted pretreatment was Der1, which was calculated using nine data points and smoothed using Savitzky and Golay polynomial smoothing on nine data points for the whole data set. L-Glu and GABA shared the same spectral pretreatment, probably due to their similar chemical structures.

The number of LVs was selected based on the minimization of the *RMSECV*, which corresponds to the predictive error obtained in the cross-validation stage. This step is similar to the cross-validation, wherein a parameter based on the division of the calibration is divided into subgroups, and each subgroup is sequentially removed for inclusion in the predictive set. The introduction of the seven LVs minimized the *RMSECV* value of GABA and L-Glu. With Der1 spectral pretreatment under seven LVs, the second batch of biotransformation samples was used as the validation set to test the stability of the PLS model (Fig. 4).

The *RPD* was used to evaluate how well the calibration model predicted compositional data. The *RPD* is defined as the *SD* of the population's reference values divided by the *RMSEP* for the NIRS calibrations. High *RPD* values indicate that the calibration model exhibits robust predictive ability. Generally, *RPD* values ranging from three to five are considered sufficient for application purposes, and the *RPD* value of five is considered to be good for quality monitoring [29]. The *RPD* values of the PLS calibration models for the GABA and L-Glu concentrations were 16.4 and 11.3, respectively (Table 3). The fitting plots of the predicted versus experimental values based on the validation set are presented in Fig. 5. These results indicate that these two calibration models can be used to reliably predict the GABA and L-Glu concentrations during the biotransformation process.

3.4. Optimization of biotransformation conditions

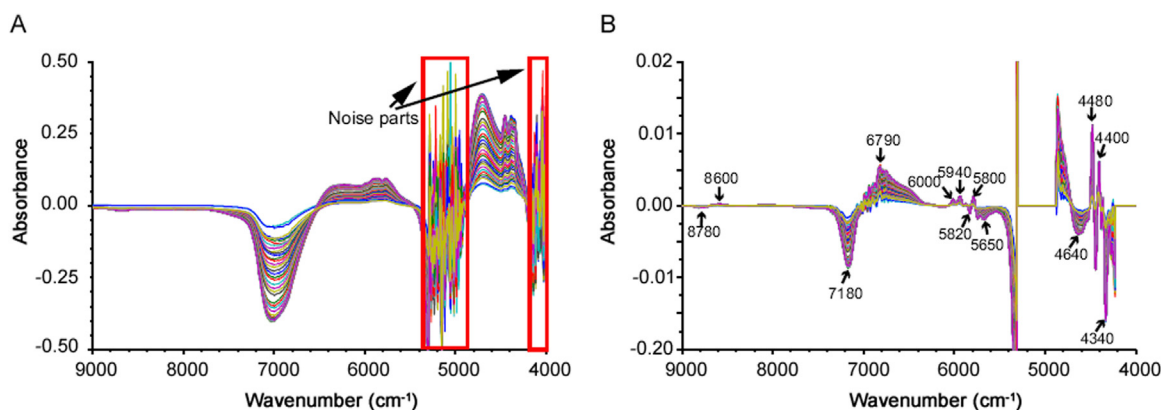The aim of the optimization of biotransformation is typically to

Fig. 3. (A) original NIR spectra and (B) Der1-preprocessed original spectra of samples taken from GABA biotransformation.

Table 3
Effects of spectral pretreatments and latent variables on the PLS models of GABA and L-Glu.

Spectral pretreatments	LVs	GABA				LVs	L-Glu			
		RMSECV (g/L)	R^2 (%)	RMSEP (g/L)	RPD		RMSECV (g/L)	R^2 (%)	RMSEP (g/L)	RPD
Raw	9	1.56	99.9	5.25	15.0	8	0.97	99.5	6.17	14.9
Constant offset elimination	9	1.47	99.9	7.07	15.1	8	0.91	99.6	6.26	15.1
Straight line subtraction	8	1.74	99.9	3.16	14.3	6	0.96	99.5	1.82	14.7
SNV	13	4.62	99.0	29.3	3.76	13	1.83	98.2	6.80	2.65
Min–max normalization	12	4.82	98.9	18.6	3.13	15	2.15	97.5	7.12	2.47
MSC	11	5.02	98.8	26.6	2.43	14	3.09	94.9	17.9	0.88
Der1	**7**	**2.02**	**99.8**	**4.00**	**16.4**	**7**	**0.95**	**99.5**	**1.62**	**11.3**
Der2	5	2.11	99.8	5.42	12.5	12	1.09	99.4	3.09	7.87
Der1+straight line subtraction	6	1.96	99.8	4.89	16.4	6	1.00	99.5	1.55	10.6
Der1+SNV	20	5.02	98.8	17.3	3.44	20	2.63	96.3	11.7	1.56
Der1+MSC	5	9.33	95.7	30.9	1.80	9	7.07	73.1	44.1	0.49

SNV: standard normal variate transformation.
MSC: multiplicative scatter correction.
Der1: first derivative.
Der2: second derivative.
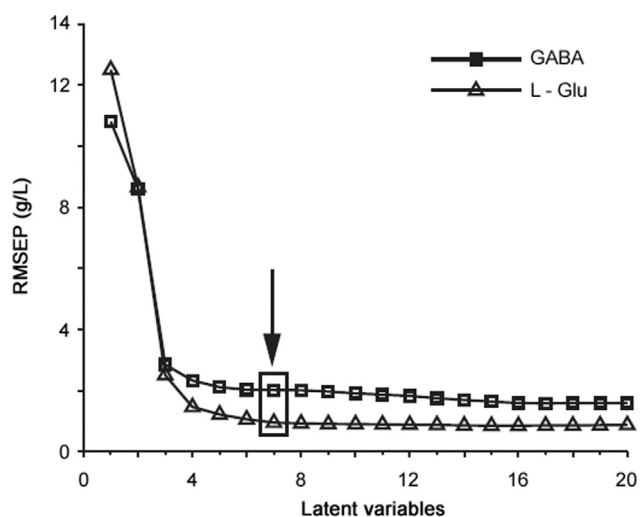The bold entry indicates the optimal spectral pretreatment (Der1).

Fig. 4. RMSEP versus the number of latent variables of the PLS regression: GABA and L-Glu.

reduce the cost and increase the production capacity within a given period of time. In this process, most of the cost came from the GAD super producer strain. Therefore, the total enzymatic activity and the conversion time were selected as the two major factors in determining the content of GABA (Y1). If the specified amount of enzyme was introduced into the reaction system in a short period of time, high initial GABA concentrations in the first hour could lead to a loss of control due to excess CO_2. Therefore, the biomass of the GAD producer strain had to be continually fed into the bioreactor to control the CO_2 production rate. The total amount of time of enzyme addition was the third factor controlling the initial GABA concentration (Y2).

According to the levels and factors of the Box-Behnken design in Section 2.8, 17 Box-Behnken design experiments were performed as listed in Table 4. The GABA content and the initial GABA concentration were predicted by the PLS model in Section 3.3.

The results of the experiments listed in Table 4 were analyzed using statistical analysis software to determine polynomial Eq. (5).

$$Y1 = 126.60 + 30.01A + 21.17B - 20.48C - 18.29AB + 22.71AC + 18.04BC - 29.52A^2 - 7.46B^2 - 6.04C^2 \qquad (5)$$

In the resulting polynomial equation, Y1 represents the response value of GABA content (g/L), while A, B and C represent three factors that influence the biotransformation process (total enzymatic activity, reaction time and total time of enzyme addition, respectively).

Terms composed of two factors represent interaction terms, and terms with second-order factors indicate the non-linear nature of the relationship between the responses and the factors. A positive sign indicates a synergistic effect, while a negative sign represents an antagonistic effect [30]. This equation indicates that
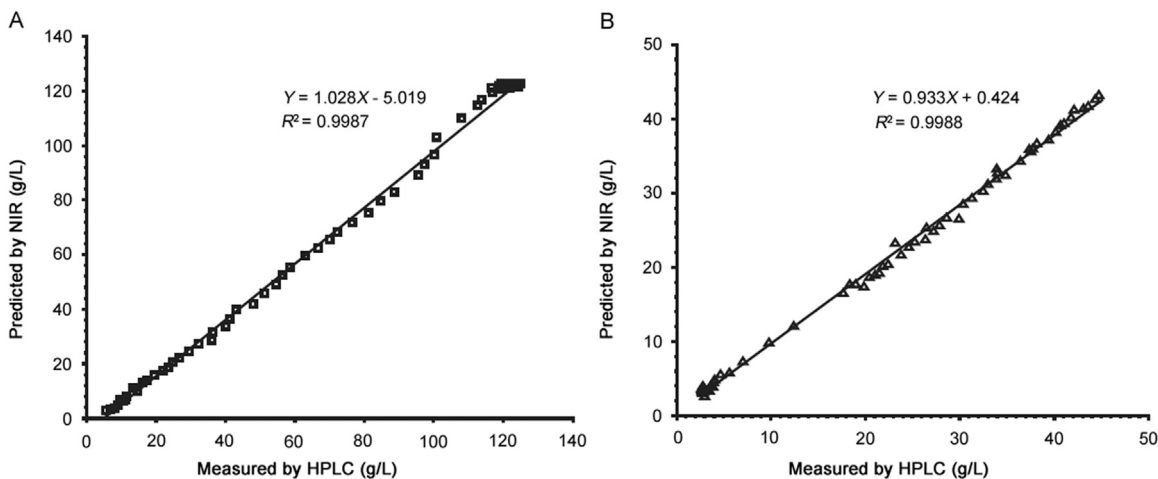
Fig. 5. Predicted versus experimental values based on the validation set: (A) GABA and (B) L-Glu.

Table 4
The Box-Behnken experimental design with responses.

No.	Total enzymatic activity (U/L)	Reaction time (h)	Total time of enzyme addition (h)	Y1: the GABA content (g/L)	Y2: the initial GABA concentration in the first hour (g/L)
1	13,320	5	3	120.62	31.38
2	3330	5	3	112.47	7.02
3	13,320	4	6	121.30	13.99
4	6660	4	3	129.40	11.98
5	13,320	4	1.5	117.22	79.03
6	6660	4	3	126.70	11.57
7	3330	4	6	17.45	5.60
8	6660	4	3	116.78	9.69
9	3330	4	3	121.40	10.28
10	3330	3	3	30.59	7.02
11	6660	4	3	115.68	13.56
12	3330	4	1.5	108.18	13.73
13	13,320	3	3	119.38	31.38
14	6660	5	1.5	128.42	27.44
15	6660	5	6	114.50	6.45
16	6660	3	6	31.38	6.45
17	6660	3	1.5	124.94	27.44

both total enzymatic activity and reaction time are positively related to the GABA content, indicating that increasing the reaction time and total enzymatic activity might increase the GABA conversion rate. The total time of enzyme addition was negatively related to the GABA content, suggesting the rate of enzyme addition could promote biotransformation. As shown in Fig. 6, increasing the enzymatic activity does not increase the GABA production. After the reaction time was fixed to 5 h, the total enzymatic activity was varied from 3330 to 13,320 U/L and the feeding time was varied from 1.5 to 6 h to optimize GABA conversion. The initial GABA concentration was held below 15 g/L during the first hour of the reaction. Enough enzyme provided at the right time can avoid the production of high levels of CO_2, improving the biological conversion efficiency. According to Eq. (5), the best condition was predicted to be 7148 U/L GAD enzymatic biomass fed in 4.33 h, with the biotransformation of L-Glu reaching the endpoint (> 99%) in the fifth hour.

3.5. Monitoring the biotransformation process using on-line NIRS model

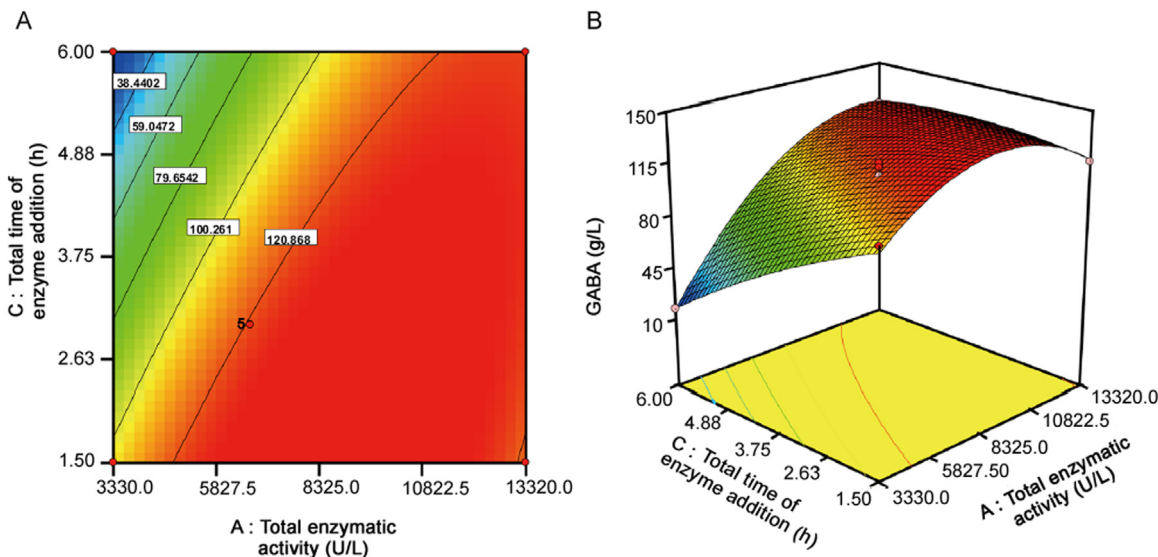To verify the reliability of the response surface model, a new batch

Fig. 6. Effects of total enzymatic activity and total time of enzyme addition on the GABA production. (A) Contour plot and (B) Response surface plot.
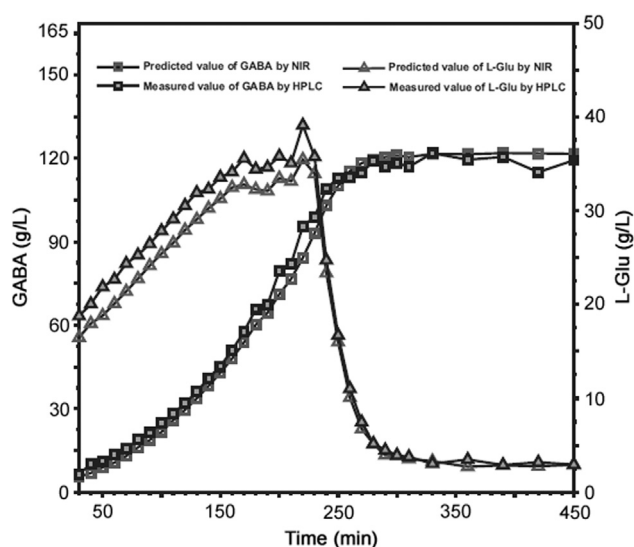
Fig. 7. Predicted and experimental values in the GABA biotransformation process.

biotransformation process was performed using the optimal parameters obtained in Section 3.4. After the first 30 min, samples were obtained every 10 min up to 450 min. The L-Glu and GABA contents were determined by the HPLC and NIRS methods, respectively.

Fig. 7 shows the predicted and true values for two different compositions during the GABA biotransformation process. The L-Glu concentration increased up to 240 min because of the constantly increasing GABA concentration, which continuously increased the pH, helping to dissolve the residual L-Glu, increasing its concentration. After 240 min, the L-Glu concentration reached its peak level, while the GABA concentration continued to steadily increase. The biotransformation catalyzed by GAD occurred without pH adjustment (pH ranged from 3.50 to 4.50), demonstrating that the GAD maintains high catalytic activity over a wide range of pH. As predicted by the response surface analysis, the reaction reached a plateau at the fifth hour, at which point the GABA concentration reached 123 g/L.

The predicted and true L-Glu and GABA concentrations exhibited similar variations over the entire biotransformation period. This demonstrated that the polynomial equations determined in the response surface analysis exhibited good predictive ability. The *RMSEP* of these equations were 1.58 and 3.07 g/L, respectively. All of these results suggest that the calibration model has a good ability to predict L-Glu (2.90–39.05 g/L) and GABA concentrations (2.01–123.41 g/L).

4. Conclusions

Monitoring the concentrations of substrates and end products in the bioreactor is important for the bioprocess control of GABA biotransformation. On-line analysis provided straightforward monitoring and rapid analysis after the samples were removed from the bioreactor. NIRS shows promise as a rapid and non-destructive method for simultaneously determining the concentrations of various compounds in the fermentation industry. Compared with traditional chemical analyses, NIRS with a PLS model is a rapid, versatile, inexpensive, and environmentally safe analytical method for predicting compound concentrations.

The results of this work demonstrate that NIRS exhibits an excellent predictive ability to monitor these concentrations in the GABA biotransformation process, with an analysis time of approximately 1 min. Therefore, on-line NIRS can be used to control and optimize fermentation processes in real time. This study combines the merits of NIRS with response surface

methodology. NIRS not only enables real-time analysis but also provides data to guide us towards the optimal biotransformation conditions determined using response surface methodology.

References

[1] I.J. Joye, L. Lamberts, K. Brijs, et al., In situ production of gamma-aminobutyric acid in breakfast cereals, Food Chem. 129 (2011) 395–401.
[2] H.Y. Kim, T. Yokozawa, T.K. Nakagawa, et al., Protective effect of gamma-aminobutyric acid against glycerol-induced acute renal failure in rats, Food Chem. Toxicol. 42 (2004) 2009–2014.
[3] S.J. Park, E.Y. Kim, W. Noh, et al., Synthesis of nylon 4 from gamma-aminobutyrate (GABA) produced by recombinant *Escherichia coli*, Bioprocess Biosyst. Eng. 36 (2013) 885–892.
[4] T. Okada, T. Sugishita, T. Murakami, et al., Effect of the defatted rice germ enriched with GABA for sleeplessness, depression, autonomic disorder by oral administration, J. Jpn. Soc. Food Sci. Technol. – Nippon Shokuhin Kagaku Kogaku Kaishi 47 (2000) 596–603.
[5] M. Shimada, T. Hasegawa, C. Nishimura, et al., Anti-hypertensive effect of gamma-aminobutyric acid (GABA)-rich chlorella on high-normal blood pressure and borderline hypertension in placebo-controlled double blind study, Clin. Exp. Hypertens. 31 (2009) 342–354.
[6] I. Cohen, V. Navarro, S. Clemenceau, et al., On the origin of interictal activity in human temporal lobe epilepsy in vitro, Science 298 (2002) 1418–1421.
[7] X. Li, Y.B. Kim, M.R. Uddin, et al., Influence of light on the free amino acid content and gamma-aminobutyric acid synthesis in *Brassica juncea* seedlings, J. Agric. Food. Chem. 61 (2013) 8624–8631.
[8] N. Komatsuzaki, J. Shima, S. Kawamoto, et al., Production of gamma-aminobutyric acid (GABA) by *Lactobacillus paracasei* isolated from traditional fermented foods, Food Microbiol. 22 (2005) 497–504.
[9] S. Lee, J. Ahn, Y.G. Kim, et al., Gamma-aminobutyric acid production using immobilized glutamate decarboxylase followed by downstream processing with cation exchange chromatography, Int. J. Mol. Sci. 14 (2013) 1728–1739.
[10] G. Macaloney, I. Draper, J. Preston, et al., At-line control and fault analysis in an industrial high cell density *Escherichia coli* fermentation, using NIR spectroscopy, Food Bioprod. Process. 74 (1996) 212–220.
[11] F. Wang, W. Jiang, C. Li, et al., Application of near infrared spectroscopy in monitoring the moisture content in freeze-drying process of human coagulation factor VIII, J. Innov. Opt. Health Sci. 8 (2015) 1793–5458.
[12] Q. Dong, H. Zang, A. Liu, et al., Determination of molecular weight of hyaluronic acid by near-infrared spectroscopy, J. Pharm. Biomed. Anal. 53 (2010) 274–278.
[13] P. Wang, H. Zhang, H. Yang, et al., Rapid determination of major bioactive isoflavonoid compounds during the extraction process of kudzu (*Pueraria lobata*) by near-infrared transmission spectroscopy, Spectrochim. Acta. A 137 (2015) 1403–1408.
[14] G. Reich, Near-infrared spectroscopy and imaging: basic principles and pharmaceutical applications, Adv. Drug. Deliv. Rev. 57 (2005) 1109–1143.
[15] P. Wang, Z. Yu, Species authentication and geographical origin discrimination of herbal medicines by near infrared spectroscopy: a review, J. Pharm. Anal. 5 (2015) 277–284.
[16] Y. Roggo, P. Chalus, L. Maurer, et al., A review of near infrared spectroscopy and chemometrics in pharmaceutical technologies, J. Pharm. Biomed. Anal. 44 (2007) 683–700.
[17] H.V. Dantas, M.F. Barbosa, E.C.L. Nascimento, et al., An automatic flow system for NIR screening analysis of liquefied petroleum gas with respect to propane content, Talanta 106 (2013) 158–162.
[18] Y.Z. Feng, D.W. Sun, Near-infrared hyperspectral imaging in tandem with partial least squares regression and genetic algorithm for non-destructive determination and visualization of Pseudomonas loads in chicken fillets, Talanta 109 (2013) 74–83.
[19] M. Blanco, R. Cueva-Mestanza, A. Peguero, NIR analysis of pharmaceutical samples without reference data: improving the calibration, Talanta 85 (2011) 2218–2225.
[20] G.W. Moncada, M.I. González Martín, O. Escuredo, et al., Multivariate calibration by near infrared spectroscopy for the determination of the vitamin E and the antioxidant properties of quinoa, Talanta 116 (2013) 65–70.
[21] S.A. Arnold, R. Gaensakoo, L.M. Harvey, et al., Use of at-line and in-situ near-infrared spectroscopy to monitor biomass in an industrial fed-batch *Escherichia coli* process, Biotechnol. Bioeng. 80 (2002) 405–413.
[22] Z.S. Wu, Y.F. Peng, W. Chen, et al., NIR spectroscopy as a process analytical technology (PAT) tool for monitoring and understanding of a hydrolysis process, Bioresour. Technol. 137 (2013) 394–399.
[23] Q. Wang, Y. Xin, F. Zhang, et al., Enhanced γ-aminobutyric acid-forming activity of recombinant glutamate decarboxylase (gadA) from Escherichia coli, World J. Microbiol. Biotechnol. 27 (2011) 693–700.
[24] H.Y. Cen, Y. He, Theory and application of near infrared reflectance spectroscopy in determination of food quality, Trends. Food. Sci. Technol. 18 (2007)

72–83.

[25] W.L. Li, L.H. Xing, Y. Cai, et al., Classification and quantification analysis of *Radix scutellariae* from different origins with near infrared diffuse reflection spectroscopy, Vib. Spectrosc. 55 (2011) 58–64.

[26] W.L. Li, Y.F. Wang, H.B. Qu, Near infrared spectroscopy as a tool for the rapid analysis of the Honeysuckle extracts, Vib. Spectrosc. 62 (2012) 159–164.

[27] E. Szłyk, A. Szydłowska-Czerniak, A. Kowalczyk-Marzec, N.I.R. spectroscopy and partial least-squares regression for determination of natural α-tocopherol in vegetable oils, J. Agric. Food. Chem. 53 (2005) 6980–6987.

[28] X. Xiao, Y.Y. Hou, J. Du, et al., Determination of main categories of components in corn steep liquor by near-infrared spectroscopy and partial least-squares regression, J. Agric. Food. Chem. 60 (2012) 7830–7835.

[29] D. Cozzolino, M.J. Kwiatkowski, M. Parker, et al., Prediction of phenolic compounds in red wine fermentations by visible and near infrared spectroscopy, Anal. Chim. Acta 513 (2004) 73–80.

[30] R.F. Xie, Z.N. Shi, Z.C. Li, et al., Optimization of high pressure machine decocting process for Dachengqi Tang using HPLC fingerprints combined with the Box–Behnken experimental design, J. Pharm. Anal. 5 (2015) 110–119.